Agronomy Research **18**(X), xxx–ccc, 2020
https://doi.org/10.15159/AR.20.165

Combustion and emission studies of a common-rail direct injection diesel engine with various injector nozzles

M. Hissa*, S. Niemi and A. Niemi

University of Vaasa, School of Technology and Innovations, P.O. Box 700, FI-65101 Vaasa Finland
*Correspondence: Michaela.Hissa@univaasa.fi

Abstract. Fuel injection has a critical role in an internal combustion engine and a significant effect on the quality of the fuel spray. In turn, fuel spray directly affects an engine´s combustion, efficiency, power and emissions. This study evaluated three different injector nozzles in a high-speed, non-road diesel engine. It was run on diesel fuel oil (DFO) and testing was conducted at three different engine loads (100%, 75% and 50%) and at two engine speeds (2,200 rpm and 1,500 rpm). The nozzles had 6, 8 and 10 holes and a relatively high mass flow rate (HF). The study investigated and compared injection and combustion characteristics, together with gaseous emissions. The combustion parameters seemed to be very similar with all studied injector nozzles. The emission measurements indicated general reductions in hydrocarbons (HC), carbon monoxide (CO) and nitrogen oxides (NOx) at most load/speed points when using the 6- and 10-hole nozzles instead of the reference 8-hole nozzles. However, smoke number increased when the alternative nozzles were used.

Key words: diesel engine, fuel injection, injector nozzle, combustion performance, emissions.

INTRODUCTION

The European Parliament has set three key targets for more efficient energy use: improve energy efficiency by 35%; increase the share of renewables in energy consumption to at least 35%; and ensure that at least 12% of energy in transport comes from renewable sources (European Parliament, 2018). The deadline to achieve all three targets is 2030, so, coupled with changing fuel prices and fuel availability issues, significant shifts in the fuel market can be expect during the next decade. Diesel engines and their injection systems in the future must be capable of handling various alternative fuels as efficiently as possible.

When modifying a diesel engine to suit new fuels, one of the most critical elements is fuel injection. It has a key role in the optimisation of the trade-off between thermal efficiency and exhaust emissions (Jääskeläinen, 2017; Heywood, 2018; Salvador et al, 2018). The injection system has a significant impact on the duration of both fuel injection and combustion, as well as combustion noise (Salvador et al, 2018). Moreover, the injector nozzle´s design - the number of nozzle holes, the hole diameter and the spray angle - affects spray atomisation and fuel-air mixing (Sarvi et al., 2008; Jääskeläinen, 2017; Dong et al., 2018a). Fuel atomisation and fuel-air mixing must improve to meet

the EU's energy efficiency target and more stringent emission regulations, including those for nitrogen oxides (NOx) (Salvador et al., 2018).

The injector nozzle is responsible for delivering the fuel spray. The injected spray consists of fuel droplets smaller than the nozzle hole diameter (Sarvi et al., 2008). Reducing nozzle hole diameter has been shown to improve atomisation efficiency, leading to increased heat release rate (HRR) and less soot formation (Sarvi et al., 2008; Jääskeläinen, 2017; Dong et al., 2018a). However, those studies found that there are limits to the reduction of nozzle diameter. These are related to total injection time and combustion durations (especially at high loads) or the potential for nozzle coking. Additionally, the accelerated combustion leads to rising combustion temperature that increases NOx emissions (Satyanarayana & Muraleedharan, 2012). NOx formation in the combustion chamber is related to the flame area, which depends on the number and size of the fuel nozzle holes (Sarvi et al., 2008; Dong et al., 2018a). Decreasing the number of holes gives a smaller cone angle of fuel spray, changing the fuel/air mixing and reducing NOx production.

If nozzle hole diameter is reduced it is necessary to increase injection pressure or raise nozzle hole count to maintain the same fuel injection rate and nozzle flow area for maximum engine torque, power objectives and engine efficiency (Jääskeläinen, 2017). Jääskeläinen (2017) states that coupling hole size reduction to several other factors may improve combustion characteristics, like reducing the potential for overlapping of the burning zones of individual fuel sprays. These factors are: injection pressure increase, changes in combustion chamber design, improvements in nozzle flow performance and increase in the number of nozzle holes.

Increasing the number of nozzle holes, however, affects the fuel penetration length. Sayin et al. (2013), reported that raising the hole count could lead to poor combustion efficiency, mainly because the shorter penetration weakens the fuel/air mixing. Lee et al. (2010) noticed a decrease in penetration length when the hole count was raised. That led to a reduction in cylinder pressure and HRR, despite the improved evaporation and atomisation.

Overall, the optimal injector nozzle parameters depend on the engine type and have to be found by testing, since there is no theory that properly describes nozzle performance (Sarvi et al., 2008). Furthermore, the suitability for each fuel has to be studied individually (Niemi et al., 2011).

The present study compares three different injector nozzles in a high-speed, non-road diesel engine powered by DFO fuel. Tests were carried out at three different engine loads (100%, 75%, 50%) and at engine speeds of 2,200 rpm and 1,500 rpm. The nozzles had 6, 8 and 10 holes and a relatively high mass flow rate (HF). No other modifications were made to the engine components or control settings. Engine performance was kept constant. Detailed injection and combustion characteristics and gaseous emissions were measured. The injection map was optimized for the reference 8-hole nozzles and the map was kept constant with the other nozzles.

The study´s main aim was to evaluate how the selected fuel nozzles affect the combustion and emission characteristics of a modern high-speed, common-rail diesel engine using commercial low-sulphur DFO. The measurements generated new information relating to nozzle choice, supporting the aim to increase efficiency of high-speed non-road engines.

MATERIALS AND METHODS

Experimental setup

The experiments were conducted by the University of Vaasa (UV) at the Internal Combustion Engine (ICE) laboratory of the Technobothnia Research Centre in Vaasa, Finland. The laboratory is managed by Novia University of Applied Sciences.

Engine setup and nozzles

The experimental engine, an AGCO Power 44 CWA, was a turbocharged, high-speed four-cylinder diesel engine for non-road applications. It was intercooled (air-to-water) and had a Bosch common-rail fuel-injection system. The engine had no exhaust after treatment devices. It was loaded by means of a Horiba eddy-current dynamometer WT300. Table 1 lists the engine´s main specification.

Testing was conducted at three different engine loads (100%, 75%, 50%) and at two engine speeds of (2,200 rpm and 1,500 rpm). Three solenoid-driven injector nozzles were compared. The nozzles had 6, 8 and 10 holes and a high mass flow rate (1.2 L min^{-1} at 100 bar). The spray angle (umbrella angle) was 149° for all nozzles. Most diesel combustion systems include spray angles in the range of 145−158° (Salvador et al., 2018). The injection map was optimised for the 8-hole nozzles by the engine manufacturer. The map was kept constant with the other nozzles. Fig. 1 and Table 2 provide detailed information about the nozzles.

The fuel used was a commercial low-sulphur diesel fuel oil (DFO). It had a cetane number (CN) of 54, lower heating value of 43 MJ kg^{-1}, its was density 835 kg m^{-3} and kinematic viscosity 3 mm^2 s^{-2}.

Table 1. Main engine specifications

Engine	AGCO POWER 44 CWA
Cylinder number	4
Bore (mm)	108
Stroke (mm)	120
Swept volume (dm^{-3})	4.4
Rated speed (min^{-1})	2,200
Rated power (kW)	96
Intermediate speed (min^{-1})	1,500

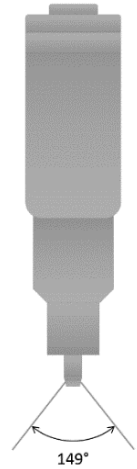

Figure 1. Spray angle schematics of the injector nozzles.

Table 2. Specifications of different injector nozzles

Number of nozzle holes	6	8	10
Orifice diameter (mm)	0.2	0.162	0.139
Total orifice areas (mm^2)	0.188	0.165	0.152
Included spray angle	149°	149°	149°
Nozzle flow rate (L min^{-1}) at 100 bar	1.2	1.2	1.2
Needle lift (mm)	0.4	0.4	0.4

Analytical instruments

LabVIEW system-design software was used to collect sensor data from the engine. The recorded variables were engine speed and torque, cylinder pressure and injection timing, duration and quantity. WinEEM3 diagnostic and service software provided by the engine manufacturer, AGCO Power, controlled fuel injection according to load-speed requests. The basic settings of WinEEM3 were the same for all nozzles and fuels. Fig. 2 depicts a schematic of the test bench setup.

Injected fuel mass flow rate was measured with a Kern digital fuel scale for 300 seconds at every load point once engine operation was stabilised. The average result was saved via LabVIEW software. The relative uncertainty for fuel mass flow measurement was 0.03%.

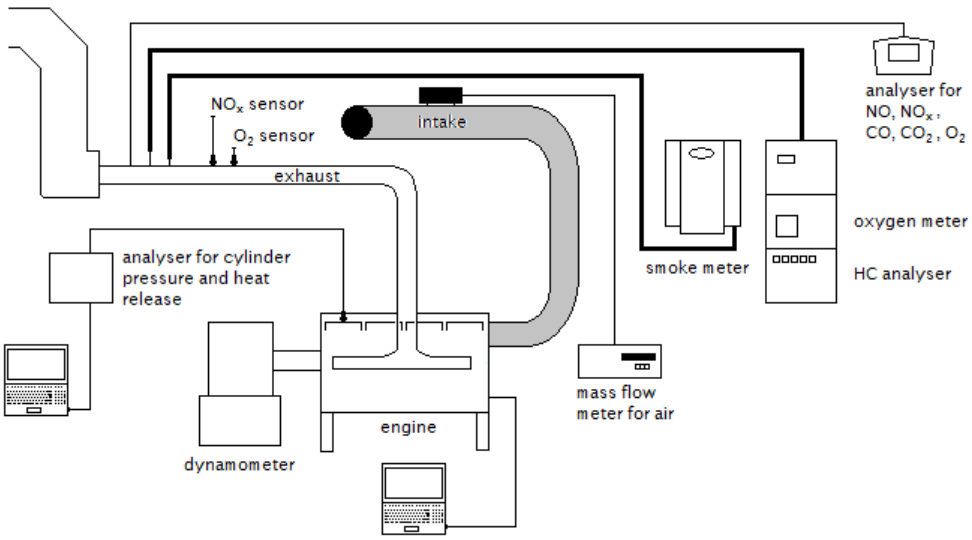

Figure 2. Engine measurement setup.

A piezoelectric Kistler 6125C pressure sensor was used to measure in-cylinder pressure. The sensor was mounted into the head of the fourth cylinder. A charge amplifier filtered and amplified the signal, which was then transmitted to a Kistler KIBOX combustion analyser. The crankshaft position was recorded by a crank-angle encoder (Kistler 2614B1), which can output a crank-angle signal with a resolution of 0.1° CA by means of an optical sensor. Cylinder pressure data were averaged over 100 consecutive cycles to smooth irregular combustion. The averaged data were used to calculate HRR. The raw data over 100 cycles were used to calculate the standard deviations for the maximum cylinder pressures.

HRR and MFB were calculated via AVL Concerto's data-processing platform, using the Thermodynamics2 macro. The macro used a calculation resolution of 0.2 °CA. The start of the calculation was set at -30 °CA. Data were filtered with the DigitalFilter macro and a frequency of 2,000 Hz. For HRR results, the average values of in-cylinder pressure were calculated first. Thereafter, the macro calculated HRR values. Finally, the HRR curve was filtered. In contrast, for MFB results, pressure values were first filtered

and then the macro was used. Average values of 100 cycles were not used for MFB results, thus establishing the standard deviations.

Exhaust temperatures were recorded by K type thermocouples (NiCu-NiAl). Air and exhaust pressures were determined by industrial transmitters. Engine air-flow was measured by an ABB Sensyflow FMT700-P air mass flow rate meter. Exhaust emissions were determined by means of the instruments listed in Table 3.

Table 3. Instruments for emission measurements

Parameter	Analyser	Technology	Accuracy*
CO	TSI CA-6203 CA-CALC	Electrochemical	0−100 ppm: ± 10% 100−5,000 ppm: ± 5%
O2	Siemens Oxymat 61	Paramagnetic	± 0.25%
NO, NOx	TSI CA-6203 CA-CALC	Electrochemical	0−100 ppm: ± 10% 100−4,000 ppm: ± 5%
HC	J.U.M. VE 7	HFID	0−100,000 ppm: ± 1%
Smoke	AVL 415 S	Optical filter	± 5%

* Accuracy provided by manufacturer.

Experimental matrix and measurement procedure

All measurements were performed under steady operation conditions without engine modifications. The comparison of injector nozzles used six load/speed points from the ISO 8178-4 standard: 100%, 75%, 50% loads at engine speeds of 2,200 rpm and 1,500 rpm. Brake mean effective pressure (BMEP) values ranged from 17.4 to 5.7 bar. The load/speed points are listed in Table 4.

Table 4. Engine operating conditions

Engine speed (rpm)	2,200			1,500		
BMEP (bar)	11.4	8.6	5.7	17.4	13.1	8.7
Load (%)	100	75	50	100	75	50

At the beginning of every measurement, the engine was warmed-up and the load was applied. The intake-air temperature was adjusted to 85 ± 1 °C downstream of the charge-air cooler to support auto-ignition of the fuels at each load. The temperature was controlled manually by regulating the flow of cooling water to the heat exchanger. The valve setting was kept constant. Therefore, the charge temperature changed with the load. All measurements were taken after the engine had stabilised, as determined by the stability of the temperatures of coolant water, intake air and exhaust upstream the turbine.

RESULTS AND DISCUSSION

Injector nozzles

The measurement results from the three injector nozzles were compared. The nozzles had 6, 8 and 10 holes but each had the same mass flow rate of 1.2 L min^{-1} at 100 bar. The rail pressure values of 8-hole nozzles were 83, 74, 66 MPa at measurement points of 11.4, 8.6 and 5.7 bar 2,200 rpm. Respectively, 61, 46 and 40 MPa at 17.4, 13.1 and 8.7 bar BMEP 1,500 rpm. The 6- and 10-hole nozzles had a minor increase in rail pressures. The maximum rail pressure increase was 4% with 6-hole nozzles at medium load (8.6 bar BMEP) at 2,200 rpm compared to rail pressure with 8-hole nozzles. The

following sections provide results and discussion from the measurements of injection timing, specific fuel consumption, heat release rate and cylinder pressure, brake thermal efficiency, mass fraction burned and combustion duration as well gaseous emissions and smoke.

Injection timing and brake specific fuel consumption

For all test conditions, pilot injections were set before top dead centre (BTDC) while main injections occurred after top dead centre (ATDC). The exact timings and durations are shown in Table 5. Fig. 3 depicts brake specific fuel consumption (BSFC).

Only main injections occurred at load points of 11.4 bar and 8.6 bar BMEP (engine speed 2,200 rpm). At this engine speed, pilot injections occurred only with the lowest BMEP of 5.7 bar (50% load). The timing and duration of these pilot injections were similar for all the nozzles. The main injection duration was slightly shorter (by just one crank angle degree) with the 8-hole nozzles. There was no post injection for any of the three loads at 2,200 rpm.

Pilot injection was used for all the nozzles at all loads (17.4, 13.1 and 8.7 bar) at the lower engine speed of 1,500 rpm. Minor variations of starting times and durations were noticed. At full load (17.4 bar) at this engine speed, post injection occurred only with the 8-hole nozzles. Post injection occurred with all the nozzles at the two smaller loads at 1,500 rpm.

Table 5. Injection timing

Nozzle	BMEP	Pilot Injection (BTDC)		Main injection (ATDC)		Post injection (ATDC)	
		Start	Duration	Start	Duration	Start	Duration
	bar	°CA	°CA	°CA	°CA	°CA	°CA
6	11.4	8.6	0	4	21	31	0
8		8.6	0	4	20	30	0
10		8.6	0	4	21	31	0
6	8.6	7.6	0	3	17	28	0
8		7.6	0	3	16	27	0
10		7.6	0	3	17	28	0
6	5.7	13	4	3.5	12	22	0
8		13	4	3.5	12	22	0
10		13	4	3.5	12	22	0
6	17.4	8.3	2.8	2.4	25	31	0
8		8	2.8	2	24	31	2.2
10		8.3	2.8	2.4	24	31	0
6	13.1	8.6	3.2	2.3	20	28	3.1
8		8.5	3.3	2.1	20	27	3.1
10		8.6	3.2	2.3	21	28	3.1
6	8.7	8.7	3.5	2.1	13	21	4.5
8		8.7	3.7	1.9	12	20	4.7
10		8.7	3.5	2.1	13	21	4.6

The amount of injected fuel was assumed to correlate to injection durations because fuel injection was controlled according to load/speed requests. Overall, the differences in main injection durations of all the nozzles did not exceed 1 °CA.

As expected, pilot injection duration increased when the engine load was reduced and main injection duration increased when the engine load was raised. At 1,500 rpm, post injection duration increased when the engine load was reduced. A longer pilot is used to shorten the ignition delay (ID) of a fuel by increasing in-cylinder temperatures for main injections. Post injections, in turn, are used to reduce particulate and soot emissions, primarily at lighter loads and lower engine speeds (Heywood, 2018).

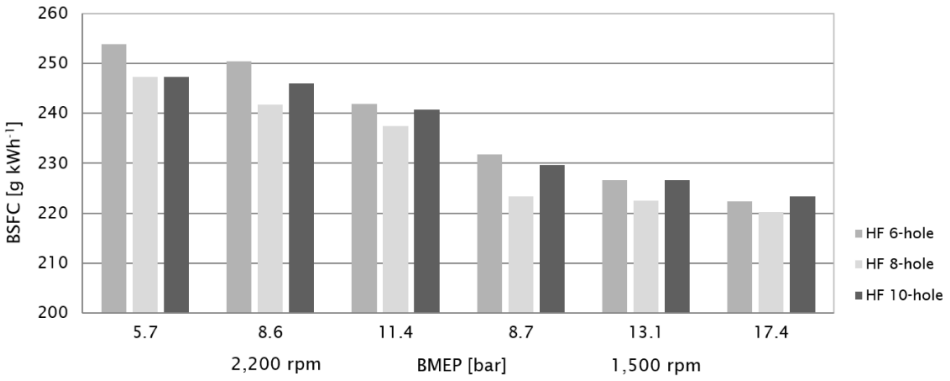

Figure 3. Brake specific fuel consumption at rated and intermediate speeds.

Brake specific fuel consumption (BSFC) is the fuel flow rate per hour (g h^{-1}) divided by engine brake power (kW). Generally, BSFC decreased when brake mean effective pressure (BMEP) or load of the engine increased. The 8-hole nozzles produced the lowest BSFC at five out of the six load/speed points. In other words, either raising the hole count to 10 or reducing it to 6 increased BSFC. The highest BSFC values were measured for the 6-hole nozzles at all load/speed points, except at full load at 1,500 rpm, where BMEP was at its maximum value of 17.4 bar. At this point, however, the difference between the 10-hole and 8-hole nozzles was minor (3.1 g kWh^{-1}, 1.4%). The maximum difference was 8.7 g kWh^{-1} or 3.6% at 8.6 bar BMEP, between the 6-hole and 8-hole nozzles.

Sayin et al. (2013) investigated 2-, 4-, 6- and 8-hole nozzles in a single-cylinder diesel engine using DFO. They also observed that increasing or decreasing the number of nozzle holes increased BSFC compared to the original nozzle. They assumed that a reduction in hole count led to enlarged fuel droplets and lengthened the ignition delay period, increasing BSFC. Conversely, raising the hole count shortened the ID period, reducing homogeneous mixture, and so once again BSFC increased. Mekonen et al. (2020) studied 3-, 4- and 5-hole nozzles in a single-cylinder diesel engine using preheated palm oil methyl ester. They observed decrease in BSFC when nozzle hole number increased from 3 to 4, due to increased fine droplets of injected fuel and improved fuel atomisation. However, BSFC increased when the nozzle hole count was raised further, from 4 to 5. They assumed that was caused by the higher number of fine droplets leading to a shorter ID and hence increasing the chance of non-homogeneous mixing.

Heat release rate (HRR)

The compression pressure was at its maximum at 2°CA before top dead centre at an engine speed of 1,000 rpm. This had no effect on measurement results, but must be considered when the results are examined.

Combustion starts with a rapid burning phase that lasts only a few CA degrees and produces the first spike in the heat release rate curve. It is followed by the main heat release period, which has a longer duration and more rounded profile. The HRR curve´s tail is the remainder of the fuel's chemical energy released when burnt gases mix with excess air that was not involved in the main combustion (Heywood, 2018). Fig. 4 shows HRR curves for the studied injector nozzles. The small dip near the beginning of each curve is the loss due to the heat transfer into the liquid fuel for vaporising and heating (Heywood, 2018).

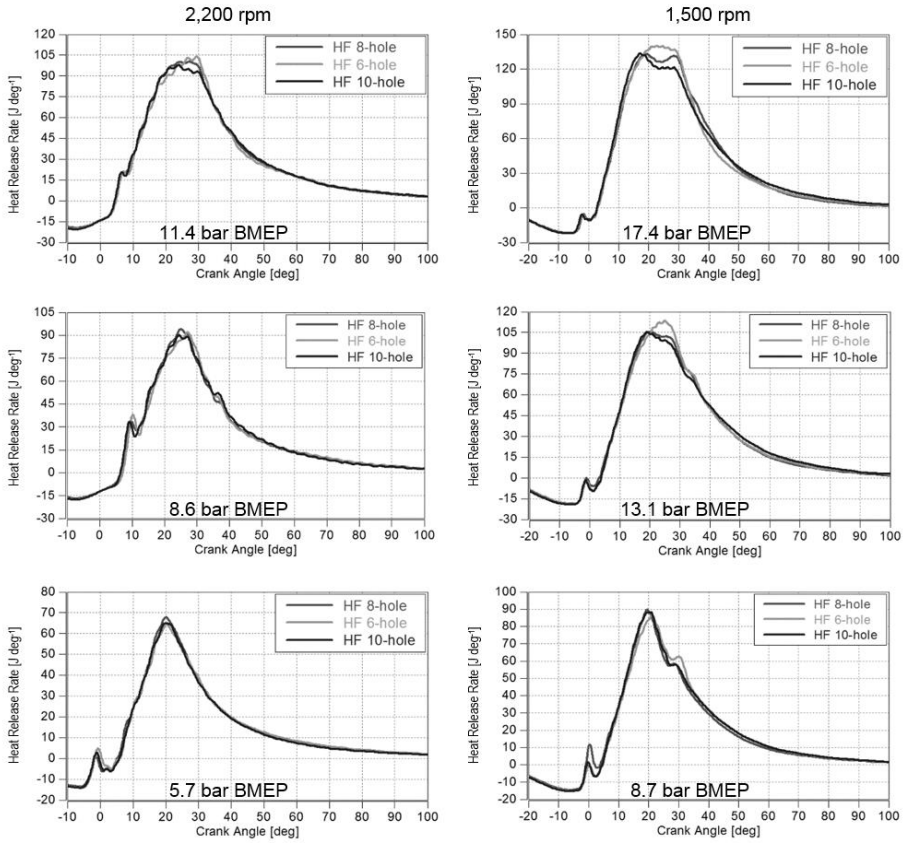

Figure 4. Heat release rates at rated and intermediate speeds.

At rated speed (2,200 rpm) and full load (11.4 bar BMEP), the maximum HRR for the 6-hole nozzles was 104 J °CA^{-1}, just before the start of post injection (27 °CA). The 10-hole nozzles´ maximum HRR peak (98 J °CA^{-1}) came earlier, at the end of main injection (24 °CA). This difference in the arrival of the HRR peak may be due to the larger droplet sizes created by the 6-hole nozzles evaporating more slowly than the

smaller droplet sizes from the 10-hole nozzles. The start of all injections, as well as injection durations, were similar for the 6- and 10-hole nozzles.

A slightly longer ignition delay observed for the 6-hole nozzles at medium (8.6 bar BMEP) and low (5.7 bar BMEP) loads is due to larger droplet size generated by larger nozzle hole diameter. Otherwise, the HRR curves are similar. The 8-hole nozzles achieved a higher HRR than the other two nozzles at medium and low loads (94 J $°CA^{-1}$ and 68 J $°CA^{-1}$ respectively).

At intermediate speed and full load (17.4 bar BMEP), only the 8-hole nozzles had a post injection, although this is not evident on the HRR curve. The curve of the 6-hole nozzles differs from those of the other two nozzles at peak HRR.

At high loads, the maximum HRR decreased as the nozzle-hole count rose. Maximum HRR occurred later at intermediate speed with the 6-hole nozzles due to the larger droplet size generated by the greater hole diameter. Additionally, this delayed HRR peak with the 6-hole nozzles also may be due to increased spray penetration length, decreased cone angle and the slower mixing that is the consequence of the larger fuel droplets´ longer evaporation time (Hoang, 2019), combined with slightly increased BSFC or fuel amount. Lee et al. (2010) studied 6-, 8- and 10-hole nozzles in a diesel engine and noticed that the strongest penetration of liquid spray from 6-hole nozzles impinged against the piston bowl, lowering in-cylinder temperature. Without the impingement, the HRR of the 6-hole nozzles should be the highest due to less uniform fuel/air distribution that enhanced combustion. They also observed the lowest HRR values for the 10-hole nozzles due to incomplete combustion caused by the poorly distributed fuel/air mixture and the highest concentration of unburned fuel during combustion process.

Cylinder pressure

Maximum cylinder pressures (MCP) were very similar with all injector nozzles at all studied load/speed points (Fig. 5 and Table 6). MCP at rated speed and full load with all nozzles were 106 to 108 bar. At 1,500 rpm, MCP at full load was 116 to 117 bar. Table 6 shows the standard deviations of MCP of 100 consecutive cycles.

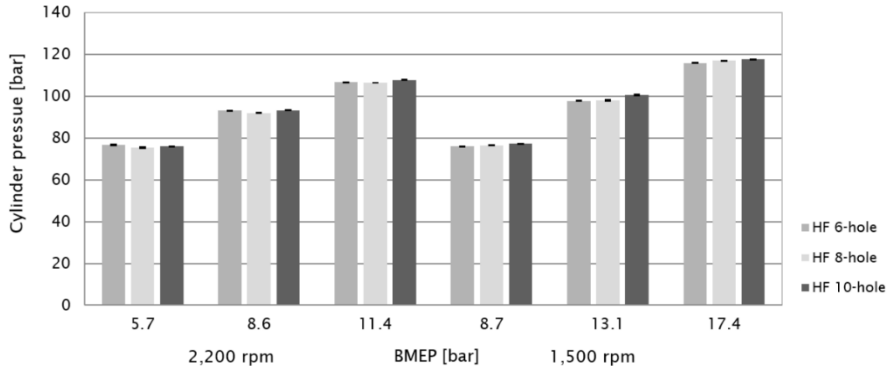

Figure 5. Maximum cylinder pressures at rated and intermediate speed with standard deviations.

Maximum cylinder pressure depends on the burned fuel fraction during the premixed combustion phase. A larger amount of fuel burned in premixed phase shows a higher MCP (Hissa et al., 2019). The fuel/air mixing rate mainly controls the combustion process of diesel engines. Slowing the rate results in retarded ignition and lower MCP. Dong et al. (2018b) noticed a lower pressure peak with a reduced number of nozzle holes, mainly due to the slower fuel/air mixing rate. In turn, Lee et al. (2010) noticed shorter penetration length when the number of nozzle holes was increased. This led to lower cylinder pressure and HRR, despite the improved evaporation and atomisation.

Table 6. Maximum cylinder pressure and standard deviations

Nozzle	BMEP bar	Max. cylinder pressure (avg) °CA	StDev	Nozzle	BMEP bar	Max. cylinder pressure (avg) °CA	StDev
6	11.4	107	0.135	6	17.4	116	0.165
8		106	0.150	8		117	0.147
10		108	0.173	10		117	0.189
6	8.6	93.0	0.114	6	13.1	97.7	0.179
8		91.9	0.140	8		97.9	0.209
10		93.1	0.133	10		100	0.264
6	5.7	76.6	0.251	6	8.7	75.9	0.154
8		75.4	0.192	8		76.4	0.237
10		76.0	0.187	10		77.2	0.158

Brake thermal efficiency (BTE)

BTE indicates how efficiently the energy in the fuel was converted into mechanical output. BTE increased with load for all nozzles due to relative reductions in heat and mechanical losses at higher load (e.g., Perumal et al., 2017). Fig. 6 shows BTE was very similar with different nozzles. At full load at 2,200 rpm, BTE was 34 to 35% and at half load 33 to 34%. At full load at 1,500 rpm, BTE was 37 to 38% and at half load 36 to 37%. Differences between nozzles were minimal and within the measurement accuracy.

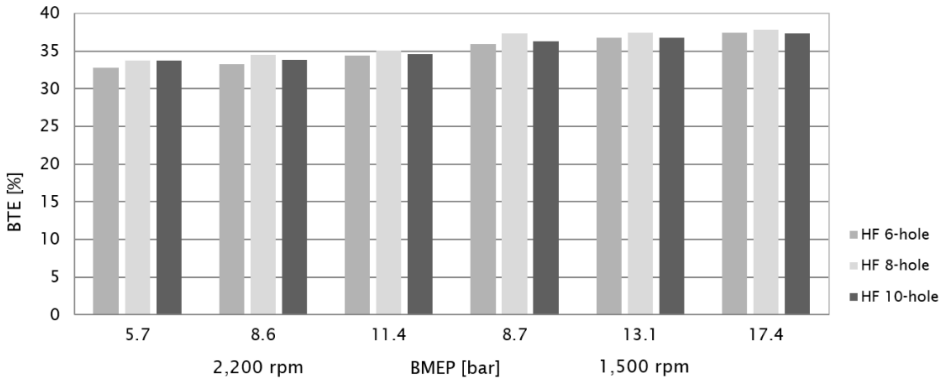

Figure 6. Brake thermal efficiency at rated and intermediate speeds.

Sayin et al. (2013) noticed an increase in BTE with higher number of nozzle holes and assumed it was because of finer atomisation of fuel. However, they also noticed an

increase in the nozzle-hole count could lead to poor combustion efficiency, mainly stemming from the shorter penetration weakening the fuel/air mixing. Mekonen et al. (2020) also measured an increased BTE when nozzle-hole number was increased from 3 to 4. This was attributed to a better fuel spray and turbulence. BTE fell when the number of nozzle holes was increased from 4 to 5. It is assumed that when the nozzle-hole count exceeds a certain range, combustion and emissions are adversely affected due to lack of the air entrainment required for the achievement of a stoichiometric mixture (Lee et al. 2010; Mekonen et al., 2020).

Mass fraction burned (MFB)

Table 7 presents MFB values with their standard deviations. It shows that the nozzles had the same MFB 5% values, except at full load at 2,200 rpm (11.4 bar BMEP) and 75% load at 1,500 rpm (13.1 bar BMEP). At these two load/speed points, the 6-hole nozzles achieved MFB 5% slightly later than the other nozzles. This may be due to increased droplet size leading to increased ID. At 50% load at 1,500 rpm (8.7 bar BMEP), the 8-hole nozzles had the earliest MFB 5%.

Table 7. Mass fraction burned and standard deviations

Nozzle	BMEP bar	MFB 5% °CA	StDev	MFB 50% °CA	StDev	MFB 90% °CA	StDev
6	11.4	19	0.14	32	0.21	65	1.0
8		18	0.15	32	0.22	63	1.1
10		18	0.13	32	0.26	64	1.3
6	8.6	20	0.14	32	0.22	67	1.1
8		19	0.15	32	0.24	65	1.2
10		20	0.11	32	0.28	64	1.1
6	5.7	17	0.17	30	0.30	67	1.6
8		17	0.16	29	0.32	65	1.6
10		17	0.16	29	0.27	64	1.3
6	17.4	14	0.13	28	0.22	55	1.2
8		14	0.11	29	0.21	53	1.0
10		14	0.14	29	0.31	58	1.5
6	13.1	16	0.15	29	0.23	58	1.3
8		15	0.13	29	0.23	56	0.94
10		15	0.15	30	0.33	61	1.1
6	8.7	16	0.17	29	0.26	58	1.2
8		15	0.13	28	0.26	56	1.1
10		16	0.12	29	0.26	58	0.97

MFB 50% values were similar with all nozzles at high loads. However, some difference between the nozzles was observed at lower cylinder pressures. At rated speed and 50% load (5.7 bar BMEP), MFB 50% of the 6-hole nozzles occurred one CA degree later than with the other nozzles. At 1,500 rpm and 75% and 50% loads (13.1 and 8.7 bar BMEP respectively), MFB 50% for the 8-hole nozzles was one CA degree ahead of the other nozzles. As a whole, differences in MFB 5% and 50% values were very small.

MFB 90% was achieved first with the 8-hole nozzles in the majority of cases. However, the 10-hole nozzles had the earliest MFB 90% values at rated speed with 75% and 50% loads (8.6 and 5.7 bar BMEP respectively). Conversely, the 10-hole nozzles

showed the latest values of MFB 90% at all loads with an engine speed of 1,500 rpm. At rated speed, the cylinder pressure and in-cylinder temperature were, perhaps, more favourable for formation, evaporation and burning of the smaller droplets from 10-hole nozzles (Chauhan et al., 2010; Hoang, 2019).

Combustion duration

Combustion duration (CD) can be defined either as the time interval between MFB 5% and MBF 50% or the time interval between MFB 5% and MFB 90%. Measurements using both definitions of CD are depicted in Fig. 7 and 8 respectively, using the data from Table 7. MFB 5% always occurred during the main injection, irrespective of nozzle or load. MFB 50% was achieved at 30 ± 2° CA. MFB 90% was observed after the end of any post injections.

CD values of MFB 5−50% were fairly similar for all the nozzles at all load/speed points, with two exceptions (Fig. 7). In the first of these, the 6-hole nozzles had a shorter CD at rated speed and full load (11.4 BMEP) because increased fuel supply at higher loads with the 6-hole nozzles enhance combustion. However, at lower loads mixing with the six-hole nozzles is poorer, ID may be delayed and combustion is more prolonged relative to the other nozzles. The second exception relates to the 10-hole nozzles; these showed longer CD values at 1,500 rpm with 75% and 100% loads (13.1 and 17.4 bar respectively). Effective fuel/air mixing with the 10-hole nozzles gave a shorter CD at low loads but at higher load CD increased, due to smaller orifice diameters that led to lengthened combustion duration. Studies of Sarvi et al. (2008), Jääskeläinen (2017) and Dong et al. (2018) stated that there is a limit to the reduction of nozzle diameter that related to e.g. total injection time and combustion durations especially at high loads.

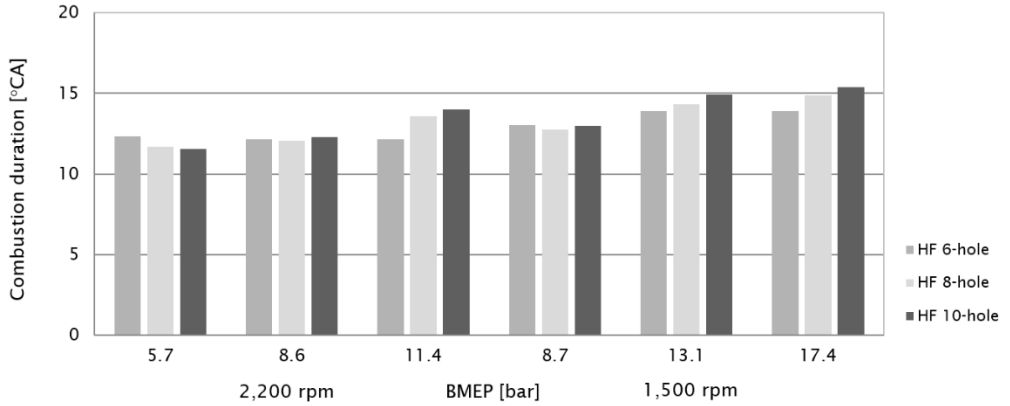

Figure 7. Combustion duration (°CA) at all engine loads, determined as crank angles between MFB 5% and MFB 50%.

Fig. 8 shows MFB 5−90% values at all load/speed points. At 2,200 rpm, the 6-hole nozzles always had the longest CD. Their larger hole diameters created larger droplets than the other nozzles; larger droplet sizes require more time to evaporate and burn (Heywood, 2018). At 1,500 rpm engine speed, the 10-hole nozzles had the longest CD and the difference compared to the other nozzles increased as engine load grew.

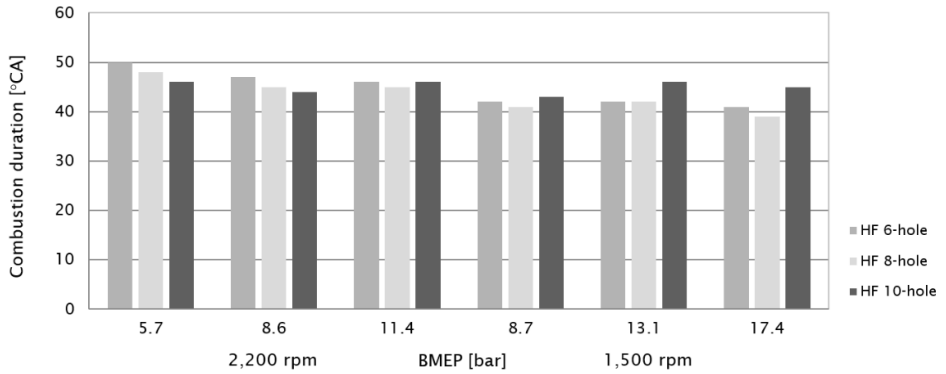

Figure 8. Combustion duration (°CA) at all engine loads, determined as crank angles between MFB 5% and MFB 90%.

Gaseous emissions and smoke

Fig. 9 illustrates the brake specific emissions of NOx, CO and HC. The smoke numbers are also depicted.

Using 6- and 10-hole nozzles instead of 8-hole nozzles generated less NOx. The 6-hole nozzles gave the lowest NOx at low loads at both speeds: 14% lower at rated speed and 18% lower at intermediate speed compared with the 8-hole nozzles. At full loads, the lowest NOx values were measured with the 10-hole nozzles. They cut NOx emissions by 11% at 2,200 rpm and by 13% at 1,500 rpm compared with 8-hole nozzles. Low smoke and high BTE indicate that combustion was efficient with 8-hole injectors, although that often is accompanied by the trade-off involving greater NOx formation. Mekonen et al. (2020) observed more NOx when they increased nozzle hole number from 3 to 4, attributing it to smaller particles that increased the combustion rate and in-cylinder gas temperature. They also measured a reduction in NOx when the nozzle number was raised from 4 to 5. The reason given was greater fuel supply to the cylinder, reducing in-cylinder gas temperature and NOx emissions. The results are consistent with the experimental observations of Lee et al. (2010) where the highest NOx emission was measured for the 8-hole nozzles. The lowest NOx values with the 10-hole nozzles were due to presence of fuel-rich zones developed from the poor mixture formation.

Carbon monoxide (CO) is mainly formed due to lack of oxygen in locally rich mixtures in the cylinder, although dissociation of CO_2 may also increase CO. The 6-hole nozzles improved CO performance at rated speed, cutting CO emissions by 20% at low load and by 39% at full load compared with the 8-hole nozzles. The 10-hole nozzles reduced CO by 15% at low load and by 19% at medium load, respectively. The 8-hole and the 10-hole nozzles produced the same amount of CO at full load. At intermediate speed, the 10-hole nozzles now produced the highest CO emissions at all load points. The increases compared with the 8-hole nozzles were considerable: 36% at low load, 26% at medium load and 83% at high load. Conversely, the 6-hole nozzles performed better than the 8-hole nozzles, reducing CO by 2%, 39% and 54% at low, medium and high loads respectively. At full load at 1,500 rpm, CO formation with 10-hole nozzles was four times higher than with the 6-hole nozzles, maybe due to the prolonged combustion. The effects of CO_2 dissociation on CO were assumed to be quite similar for all nozzles because the high temperatures prevailed in the cylinder for quite similar periods with them all.

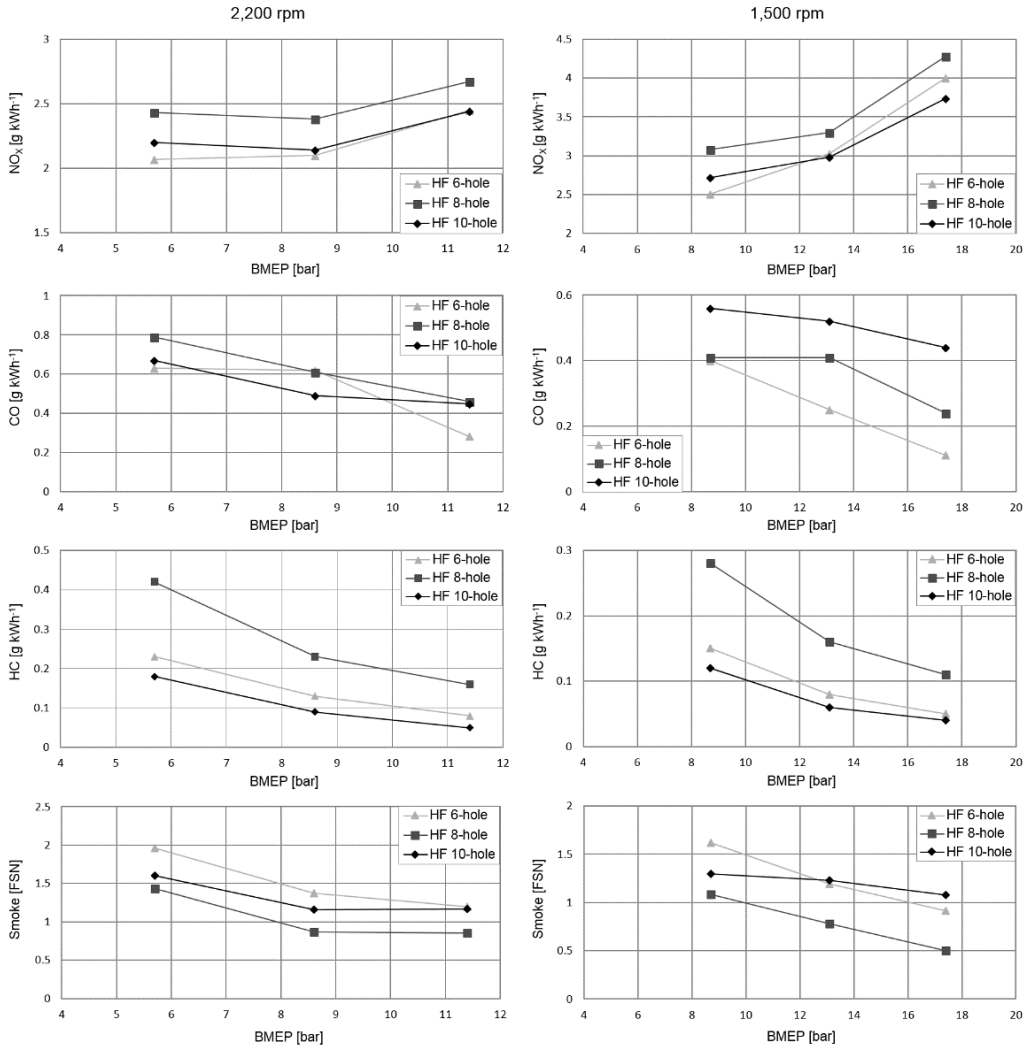

Figure 9. Brake specific emissions of NOx, CO and HC and smoke numbers versus engine load at two speeds.

Total hydrocarbon emissions (HC) are considered to reflect the presence of unburnt or partially burnt fuel in the exhaust gas (Hoang, 2019). Most exhaust HC originate from the fuel but some are formed by unknown chemical reactions within the cylinders (Satyanarayana & Muraleedharan, 2012). An increase in HC emissions is indicative of reduced thermal efficiency and a raised level of pollutants (Hoang, 2019). In our study, both the alternative nozzles gave better HC performance than the reference nozzles at all loads and speeds, with the 10-hole nozzles being slightly the most beneficial. At rated speed, the 10-hole nozzles reduced HC emissions by 57% at low load, 60% at medium load and 68% at high load compared with 8-hole nozzles. At intermediate speed, 10-hole nozzles achieved HC reductions of 57%, 62% and 63% respectively.

Exhaust smoke increased when engine load reduced. Smoke number at the engine´s rated speed was always highest with 6-hole nozzles. The smoke result was less clear-cut

at intermediate speed: the 6-hole nozzles generated the highest smoke at low load but the 10-hole nozzles produced the most smoke at the highest load. The 8-hole nozzles gave the lowest smoke at both speeds and all loads, ranging from 0.9 to 1.5 FSN at rated speed and from 0.5 to 1.1 at intermediate speed.

Sarvi et al. (2008) reported that NOx decreased when the number of nozzle holes was reduced for a given fuel consumption in a medium-speed diesel engine driven with light fuel oil (LFO). However, that was accompanied by the penalty of greater smoke (FSN), HC and CO concentrations. Dong et al., (2018a), say that combustion efficiency improves with smaller fuel droplets. Heat release is accelerated and combustion temperature rises, giving higher NOx. On the other hand, NOx formation in the combustion chamber is related to the flame area. A lower number of nozzle holes gives a smaller fuel jet area, resulting in different fuel/air mixing which reduces NOx production (Dong et al, 2018a; Sarvi et al., 2008).

Generally, NOx formation increased with engine load. Higher combustion temperature promoted NOx formation. Figure 8 shows that higher engine load improved fuel/air mixing and fuel oxidation processes. The improved mixing rate led to reductions of CO, HC and smoke when engine load was increased.

CONCLUSIONS

The present study compared three different injector nozzles in a high-speed non-road diesel engine at different engine loads and speeds. The main aim was to find out how the selected nozzles affect combustion and emission characteristics of the common-rail experimental engine, fuelled by commercial low-sulphur DFO. The nozzles had 6, 8 and 10 holes. The injection map was kept constant and the engine control module set the injection for each nozzle automatically. The measurements generated new information of fuel injection nozzles supporting the development of more efficient high-speed non-road engines.

Based on the performed measurements and analyses, the following conclusions could be drawn:

- The BSFC for the 6- and 10-hole nozzles were higher than that of the 8-hole nozzles.
- The HRRs were fairly similar for all nozzles at all loads. However, the HRR remained slightly longer at a high level with 6-hole nozzles.
- Differences in maximum cylinder pressures and BTE were minimal between the nozzles.
- Combustion durations were almost similar for all the nozzles.
- The 6- and 10-hole nozzles improved CO and HC formation.
- The 8-hole tips generated the highest NOx but lowest smoke at all loads.

ACKNOWLEDGEMENTS. This project was one part of the national Future Combustion Engine Power Plant research program. The authors wish to thank Business Finland for the financial support of the program.

The authors offer their appreciation to Dr. Katriina Sirviö, Mr. Olav Nilsson, Mr. Markus Uuppo and Mr. Teemu Ovaska for the assistance in the measurements. The authors also express their gratitude to Mr. Henri Huusko and Mr. Marko Vallinmäki at AGCO Power Inc. for their kind assistance in providing test nozzles and their specifications for the study.

REFERENCES

Chauhan, B.S., Kumar, N., Du Jun, Y. & Lee, K.B. 2010. Performance and emission study of preheated Jatropha oil on medium capacity diesel engine. *Energy* **35**, 2484−2492.

Dong, S., Wang, Z., Yang, C., Ou, B., Lu, H., Xu, H. & Cheng, X. 2018a. Investigations on the effects of fuel startification on auto-ignition and combustion process of an ethanol/diesel dual-fuel engine. *Applied Energy* **230**, 19−30.

Dong, S., Yang, C., Ou, B., Lu, H. & Cheng, X. 2018b. Experimental investigation on the effects of nozzle-hole number on combustion and emission characteristics of ethanol/diesel dual-fuel engine. *Fuel* **217**, 1−10.

European Parliament. 2018. MEPs set ambitious targets for cleaner, more efficient energy use. https://www.europarl.europa.eu/news/en/press-room/20180112IPR91629/meps-set-ambitious-targets-for-cleaner-more-efficient-energy-use. Accessed 15.1.2020.

Heywood, J.B. 2018. *Internal Combustion Engine Fundamentals*, 2nd Edition, McGraw-Hill Education, USA, 1028 pp.

Hissa, M., Niemi, S., Sirviö, K., Niemi, A. & Ovaska, T. 2019b. Combustion Studies of a Non-Road Diesel Engine with Several Alternative Liquid Fuels. *Energies* **12**, 2447.

Hoang, A.T. 2019. Experimental study on spray and emission characteristics of a diesel engine fueled with preheated bio-oils and diesel fuel. *Energy* **171**, 795−808.

Jääskeläinen, H. 2017. *DieselNet Technology Guide − Diesel Fuel Injection Nozzles*. https://dieselnet.com/tg. Accessed 20.9.2019.

Lee, B.H., Song, J.H., Chang, Y.J. & Jeon, C.H. 2010. Effect of the number of fuel injector holes on characteristics of combustion and emissions in a diesel engine. *International Journal of Automotive Technology* **11**(6), 783−791.

Mekonen, M. W. & Sahoo, N. 2020. Combined effects of fuel injection pressure and nozzle holes on the performance of preheated palm oil methyl ester used in a diesel engine. *Biofuels* **11**(1), 19−35.

Niemi, S., Uuppo, M., Virtanen, S., Karhu, T., Ekman, K., Svahn, A., Vauhkonen, V., Agrawal, A. & Hiltunen, E. 2011. Animal Fat Based Raw Bio-Oils in a Non-Road Diesel Engine Equipped with a Diesel Particulate Filter. In Bartz, W.J. (ed) (2011): *8th International Colloquium Fuels; Conventional and Future Energy for Automobiles*. Ostfildern, Germany: Technische Akademie Esslingen. pp. 517–528.

Perumal, V. & Ilangkumaran, M. 2017. Experimental analysis of engine performance, combustion and emission using pongamia biodiesel as fuel in CI engine. *Energy* **129**, 228–236.

Salvador, F.J., Lopez, J.J., De la Morena, J. & Crialesi-Esposito, M. 2018. Experimental investigation of the effect of orifices inclination angle in multihole diesel injector nozzles. Part 1 – Hydraulic performance. *Fuel* **213**, 207−214.

Sarvi, A., Fogelholm, C-J. & Zevenhoven, R. 2008. Emissions from large-scale medium-speed diesel engines: 1. Influence of engine operation mode and turbocharger. *Fuel Processing Technology* **89**, 510−519.

Satyanarayana, M. & Muraleedharan, C. 2012. Experimental Studies on Performance and Emission Characteristics of Neat Preheated Vegetable Oils in a DI Diesel Engine. *Energy Sources, Part A: Recovery, Utilization, and Environmental Effects* **34**, 1710−1722.

Sayin, C., Gumus, M. & Canakci, M. 2013. Influence of injector hole number on the performance and emissions of a DI diesel engine fueled with biodiesel-diesel fuel blends. *Applied Thermal Engineering* **61**, 121–128.